NUMERICAL SIMULATION ON THE TWO-PHASE FLOW PATTERN IN THE LOOP HEAT PIPE WITH R-134A

Seong Hyun Park, Yong Gap Park*, Man Yeong Ha
*Author for correspondence
Rolls-Royce and Pusan National University Technology Centre in Thermal Management,
Jang Jeon 2-Dong, Geum Jeong Gu, Busan 609-735
Republic of Korea
E-mail: pyg777@pusan.ac.kr

ABSTRACT

This paper discusses the two-phase flow pattern in the loop heat pipe with R-134a. A computational fluid dynamics (CFD) study was carried out using ANSYS FLUENT. VOF model was used to simulate interface between vapor and liquid phase of R-134a. A UDF was used to model evaporation and condensation mass transfer between two phases. For the simulation of increase of pressure in the loop heat pipe, the ideal gas law was considered when modelling the density of vapor. The numerically calculated temperatures in this paper and Fadhl's calculated temperatures and experimentally measured temperatures matched very well [2]. The maximum difference between the calculated and Fadhl's temperature data is 2.4 %. The bubble figure in the loop heat was observed with time passed in this paper.

INTRODUCTION

A heat pipe is a two-phase heat transfer device with a highly effective heat transfer rate through evaporating and condensing a fluid that is circulating in a sealed container [1]. The loop heat pipe uses capillary action to remove heat from a source and passively move it to a condenser. In the loop heat pipes, evaporation section and condensation section are existed. The heat enters the evaporation section by the heater and the working fluid absorbs an amount of heat proportional to the latent heat of evaporation, which is sufficient to change the fluid from liquid to vapor [2]. The vapor then flows to the condensation section, where the heat is transferred from vapor to the liquid. In the condensation section, vapor condenses and condensed liquid is then returned to the evaporator due to capillary forces. Loop heat pipe has advantages of being able to provide reliable operation over long distance and the ability to operate against gravity.

Many numerical studies are focused on the development of mathematical modelling by calculating thermal resistance of the system or 1D thermal network analysis [3-7]. The computational fluid dynamic (CFD) simulation should be conducted to understand heat and mass transfer mechanism in the heat pipe deeply. A limited number of CFD numerical simulation studies are published because CFD studies regarding multiphase flow with phase change are very computationally expensive compared to single phase problem.

NOMENCLATURE

ρ	[kg/m^3]	Density
α	[-]	Volume fraction
μ	[kg/m·s]	Viscosity
$\vec{v}$	[m/s]	Velocity
h	[J/kg]	Enthalpy
p	[Pa]	Pressure
T	[K]	Temperature
S_E	[W/m^3]	Energy source term
S_M	[kg/m^{3}s]	Mass source term
k	[m^2/s^2]	Turbulent kinetic energy
ω	[1/s]	Specific dissipation rate
L	[J/kg]	Latent heat

Subscripts

v	Vapor
l	Liquid
sat	Saturation

There are some published studies regarding multiphase flow simulations in the thermosyphon [1-2, 8-11]. A. Alizadehdakhel et al. [9] modeled a gas/liquid two-phase flow and the simultaneous evaporation and condensation phenomena in a thermosyphon. The volume of fluid (VOF) technique was used to model the interaction between these phases. For modeling of evaporation and condensation in a thermosyphon, additional equations regarding mass and momentum source were calculated proposed by S. C. K. De Schepper [8]. The numerical temperature data were validated with measurement temperature. They concluded that CFD is a useful tool to model and explain the complex flow and heat transfer in a thermosyphon.

The density considered in these papers was considered as constant value. However, in case of high pressure problem due to a large amount of heating power, pressure is increased by the supply of heating power continuously and as a result of increase of pressure in the system, the vapor in the system would be compressed. Therefore, the density of vapor would be increased as time passed. There are very limited number of papers considering the increase of vapor density during calculations [12].

In this study, a CFD study was conducted to analyze the effect of the location of heater inserted in the loop heat pipe. For the CFD study, the commercial code ANSYS FLUENT 15.0 was

used with implementation of user defined functions (UDF) to simulate evaporation and condensation of working fluid. The ideal gas law was used to consider the effect of change of vapor density. The change of saturation temperature due to the increase of pressure in the system was also considered.

NUMERICAL METHODOLOGY

The commercial code ANSYS FLUENT 15.0 was used and mass continuity, momentum, energy, turbulent and volume fraction equations were used to describe motion of bubbles and temperature field in the loop heat pipe. The Volume of Fluid (VOF) method was applied for the description of interface between vapor and liquid. In the VOF model, single momentum equation, single energy equation and single turbulent equation were solved through the computational domain and resulting velocity and temperature fields were shared among the phases. The properties appearing in the transport equations are determined by the presence of the component phases in each control volume. The volume fraction of each of the fluids in each computational cell is tracked throughout the domain by defining the volume fraction conservation equation. For the turbulent flow, a k-ω model was used. All of governing equations solved in the current study are shown below:

Volume fraction equation

$$\frac{\partial(\alpha_v\rho_v)}{\partial t}+\nabla\cdot\left(\alpha_v\rho_v\vec{v}\right)=S_M \tag{1}$$

Continuity equation

$$\frac{\partial\rho}{\partial t}+\nabla\cdot\left(\rho\vec{v}\right)=0 \tag{2}$$

Momentum equation

$$\frac{\partial}{\partial t}(\rho\vec{v})+\nabla\cdot(\rho\vec{v}\vec{v})=-\nabla p+\nabla\cdot\left[\mu\left(\nabla\vec{v}+\nabla\vec{v}^{T}\right)\right]+\rho\vec{g}+\vec{F} \tag{3}$$

Energy equation

$$\frac{\partial}{\partial t}(\rho E)+\nabla\cdot\left(\vec{v}\left(\rho E+p\right)\right)=\nabla\cdot\left(k_{eff}\nabla T\right)+S_E \tag{4}$$

$$E=h-\frac{p}{\rho}+\frac{v^2}{2} \tag{5}$$

Standard k-ω equations

$$\frac{\partial}{\partial t}(\rho k)+\nabla\cdot(\rho k\vec{v})=\nabla\cdot\left(\Gamma_k(\nabla k)\right)+G_k-Y_k \tag{6}$$

$$\frac{\partial}{\partial t}(\rho\omega)+\nabla\cdot(\rho\omega\vec{v})=\nabla\cdot\left(\Gamma_\omega(\nabla k)\right)+G_\omega-Y_\omega \tag{7}$$

The density and viscosity used in governing equations were defined as the volume-fraction-averaged value as shown following form:

$$\rho=\alpha_v\rho_v+\alpha_l\rho_l \tag{8}$$

$$\mu=\alpha_v\mu_v+\alpha_l\mu_l \tag{9}$$

In this study, the user-defined functions (UDFs) were employed to specify customized source terms proposed by S. C. K. De Schepper [8] to simulate mass source and energy source for the evaporation and condensation process. Mass source and were defined as shown below:

For mass transfer during evaporation process

$$S_{M,l}=-0.1\rho_l\alpha_l\frac{T-T_{sat}}{T_{sat}} \tag{10}$$

$$S_{M,v}=-S_{M,l} \tag{11}$$

For mass transfer during condensation process

$$S_{M,l}=0.1\rho_v\alpha_v\frac{T_{sat}-T}{T_{sat}} \tag{12}$$

$$S_{M,v}=-S_{M,l} \tag{13}$$

Eq. (10) denotes the amount of mass taken from the liquid phase and Eq. (11) denotes the amount of mass added to the vapor phase and Eq. (12) denotes the amount of mass added to the liquid phase and Eq. (13) denotes the amount of mass taken from the vapor phase. Energy source S_E are also defined to consider the latent heat of evaporation and condensation process. The energy source can be expressed as follows:

Energy source term during evaporation process

$$S_E=-0.1\rho_l\alpha_l L\frac{T-T_{sat}}{T_{sat}} \tag{14}$$

For source term during condensation process

$$S_E=0.1\rho_v\alpha_v L\frac{T_{sat}-T}{T_{sat}} \tag{15}$$

TEST GEOMETRY AND BOUNDARY CONDITIONS

The 2D CFD geometries were developed to represent the loop heat pipe as shown in Figure 1. A heater is inserted inside the loop heat pipe to generate bubble. In order to simulate the heater, a constant heat flux is defined at the wall boundaries of the evaporator section, depending on the power input. For consideration of convective heat transfer by surround air, convective boundary conditions were applied at outside walls. The heat transfer coefficient was $10\ W/m^2K$ and free stream temperature was -20℃.

The working fluid inside the heat pipe is R-134a. The vapor of R-134a inside the loop heat pipe was compressed as evaporation occurred in the heater surface. For the consideration of increase of density due to the increase of pressure in loop heat pipe, the ideal gas law applied. Other thermophysical properties such as viscosity, thermal conductivity, specific heat and density of liquid were considered as polynomial functions of temperature. To create the polynomial functions, the data were extracted with reference to the NIST database. All data were fitted with a polynomial equation.

The variation of saturation temperature is varied with pressure during calculation. The evaporation mass transfer rate

could be decreased as saturation temperature is increased. The variation of saturation temperature was considered as polynomial function of pressure. To create the polynomial functions, saturation temperature data was fitted with polynomial function.

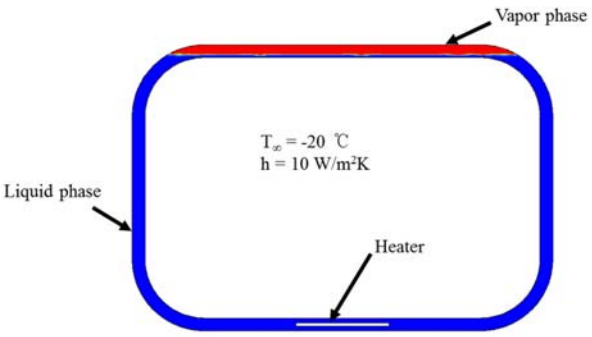

Figure 1 Computational domain and boundary conditions for CFD simulation

VALIDATION OF NUMERICAL METHODOLOGY

For the verification of CFD model used in this study, temperature distribution obtained using numerical methodology mentioned in previous chapter were compared with Fadhl's experimental and numerical temperature data [2]. Because there wasn't enough numerical and experimental papers regarding loop heat pipe, verification of numerical methodology was performed in the thermosiphon geometry. The experimental results can be employed to make comparison for the sake of validation. All the geometry and numerical conditions were same as those in the Fadhl's study. Figure 2 shows a qualitative comparison between the numerically calculated temperatures and Fadhl's calculated and experimentally measured temperature at the measured positions. The following experimental and numerical temperature discrepancy were defined for the comparison:

$$\Delta T = \frac{\left|T_{cal} - T_{\exp}\right|}{T_{\exp}} \times 100 \ (\%) \tag{16}$$

The numerically calculated temperatures in this paper and Fadhl's calculated temperatures and experimentally measured temperatures matched very well. The maximum difference between the calculated and Fadhl's temperature data is 3.6 %.

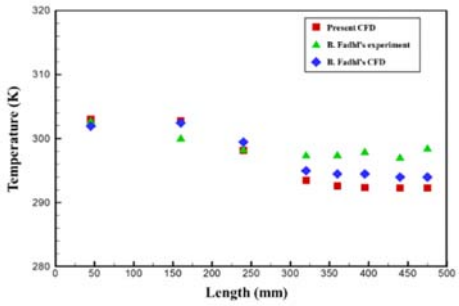

Figure 2 Comparison of temperature of numerical results with Fadhl's calculation and measurement data [2]

RESULTS

Fig. 3 shows the volume fraction distribution at the initial stage of operation in the whole heat pipe and the variation of averaged pressure of the loop heat pipe at that time. At the beginning of heating process, temperature around heater was increased by applying constant heat flux at the heater. Nucleation of bubbles occurred at the heater when the temperature at the heater surface exceed saturation temperature of R-134a. The nucleated bubbles grew as time passed and bubbles tended to move to the space between top surface of heater and wall of loop heat pipe. As a results, bubbles were aggregated at both top and bottom surface of heater between 1.2 s and 5.9 s. The vapor layer grew continuously due to the nucleation of bubbles at the heater surface. The vapor layer was separated when the length of vapor layer was longer than the length between heater and curved pipe of loop heat pipe. At 5.9 s, the vapor layer which was located between top surface of heater and curved pipe of loop heat pipe was separated into large bubbles because the bouncy force was larger than surface tension between vapor layer and loop heat pipe wall.

Large bubbles which were separated from vapor layer travelled upward and pull the liquid and top side of vapor layer to the clockwise direction between 5.8 s and 7.1 s as shown in Figure 3. The pressure was increased until 5.8 s due to the nucleation of bubbles at heater surface and then decreased rapidly due to the detachment of bubbles at 5.8 s. The top side of vapor layer moves to the right side of loop heat pipe between 6.5 s and 7.1 s because the momentum induced by left side of vapor was decreased. This procedure occurred repeatedly during the operation. The saturation temperature was increased due to the increase of pressure. The temperature difference between heater surface and saturation working fluid was decreased because the saturation temperature is increased. The evaporation mass transfer rate was proportional to the temperature difference between heater surface and saturation working fluid. Therefore, the evaporation mass transfer rate was decreased.

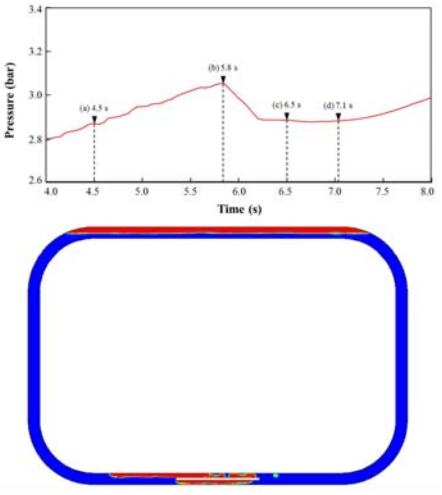

(a) 4.5 s

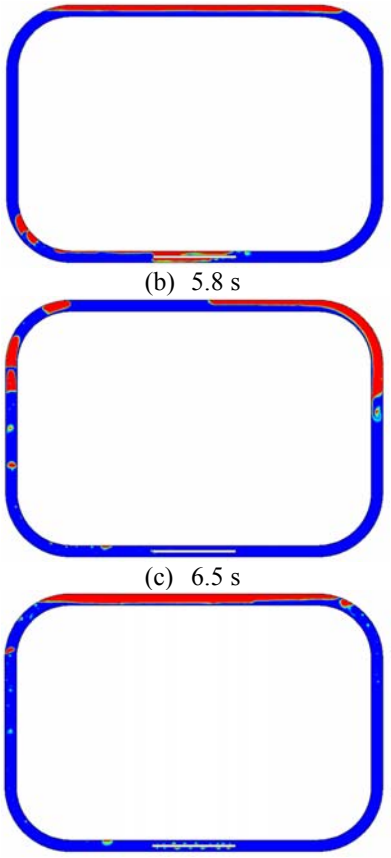

(b) 5.8 s

(c) 6.5 s

(d) 7.1 s

Figure 3 Volume fraction distribution at t = 4.5 s, 5.8 s, 6.5 s, and 7.1 s

CONCLUSION

A numerical study of loop heat pipe was carried out while considering mass transfer by evaporation and condensation process. The simulation was solved using a 2D geometry and ANSYS FLUENT. For the consideration of increase of density due to the increase of pressure in loop heat pipe, the ideal gas law applied. Other thermophysical properties of R-134a such as viscosity, thermal conductivity, specific heat, density of liquid and saturation temperature were considered as polynomial functions of temperature. The simulation results showed good agreement with the measurement data.

The simulation results showed instantaneous two-phase flow pattern including bubbles generation and movement in the loop heat pipe. Nucleation of bubbles occurred at the heater when the temperature at the heater surface exceed saturation temperature of R-134a. The nucleated bubbles grew as time passed and bubbles tended to move to the space between top surface of heater and wall of loop heat pipe. The nucleated bubble was separated when the length of vapor layer was longer than the length between heater and curved pipe of loop heat pipe. The separated bubbles circulated and condensed in the loop heat pipe.

ACKNOWLEDGEMENT

"This research was supported by Basic Science Research Program through the National Research Foundation of Korea(NRF) funded by the Ministry of Education, Science and Technology(NRF-2017R1C1B2007296)"

REFERENCES

[1] B. Fadhl, L. C. Wrobel, Hussam Jouhara, Numerical modelling of the temperature distribution in a two-phase closed thermosiphon, Applied Thermal Engineering 60 (2013) 122-131

[2] Bandar Fadhl, Luiz C. Wrobel, Hussam Jouhara, CFD modelling of a two-phase closed thermosyphon charged with R134a and R404a, Applied Thermal Engineering 78 (2015) 482-490

[3] L. M. Poplaski, A. Faghri, T. L. Bergman, Analysis of internal and external thermal resistances of heat pipes including fins using a three-dimensional numerical simulation, International Journal of Heat and Mass Transfer 102 (2016) 455-469

[4] S. Lin, J. Broadbent, R. McGlen, Numerical study of heat pipe application in heat recovery systems, Applied Thermal Engineering 25 (2005) 127–133

[5] S. Touahri, T. Boufendi, Numerical study of the conjugate heat transfer in a horizontal pipe heated by joulean effect, Numerical Study of the Conjugate Heat Transfer in a Thermal Science, 16 (2012) 53-67

[6] T. Daimaru, S. Yoshida, H. Nagai, Study on thermal cycle in oscillating heat pipes by numerical analysis, Applied Thermal Engineering 113 (2017) 1219-1227

[7] W. Qu a, H.B. Ma, Theoretical analysis of startup of a pulsating heat pipe, International Journal of Heat and Mass Transfer 50 (2007) 2309-2316

[8] S. Schepper, G. Heynderickx, G. Marin, Modeling the evaporation of a hydrocarbon feedstock in the convection section of a steam cracker, Computers and Chemical Engineering 33 (2009) 122–132

[9] A. Alizadehdakhel, M. Rahimi, A. A. Alsairafi, CFD modeling of flow and heat transfer in a thermosyphon, International Communications in Heat and Mass Transfer 37 (2010) 312–318

[10] K. Kafeel, A. Turan, Simulation of the response of a thermosyphon under pulsed heat input conditions, International Journal of Thermal Sciences 80 (2014) 33–40

[11] L. Asmaie, M. Haghshenasfard, A. Mehrabani-Zeinabad, M. N. Esfahany, Thermal performance analysis of nanofluids in a thermosyphon heat pipe using CFD modeling, Heat Mass Transfer 49 (2013) 667–678

[12] W. Kalata, K. J. Brown, R. J. Schick, Injector Study via VOF: Emphasis on Vapor Condensation due to Spray, 23rd Annual Conference on Liquid Atomization and Spray Systems (2011)

[13] W. Leia, L. Yanzhong, L. Zhana, Z. Kanga, Numerical investigation of thermal distribution and pressurization behavior in helium pressurized cryogenic tank by introducing a multi-component model, 25th International Cryogenic Conference & International Cryogenic Materials Conference (2014)